

## Dynamic analysis of slack moored spar platform with 5 MW wind turbine

T. Seebai\* and R. Sundaravadivelu

*Department of Ocean Engineering, Indian Institute of Technology Madras Chennai-600036,  
Tamil Nadu, India*

*(Received April 5, 2011, Revised November 23, 2011, Accepted December 8, 2011)*

**Abstract.** Spar platforms have several advantages for deploying wind turbines in offshore for depth beyond 120 m. The merit of spar platform is large range of topside payloads, favourable motions compared to other floating structures and minimum hull/deck interface. The main objective of this paper is to present the response analysis of the slack moored spar platform supporting 5MW wind turbine with bottom keel plates in regular and random waves, studied experimentally and numerically. A 1:100 scale model of the spar with sparD, sparCD and sparSD configuration was studied in the wave basin (30 × 30 × 3 m) in Ocean engineering department in IIT Madras. In present study the effect of wind loading, blade dynamics and control, and tower elasticity are not considered. This paper presents the details of the studies carried out on a 16 m diameter and 100 m long spar buoy supporting a 90 m tall 5 MW wind turbine with 3600 kN weight of Nacelle and Rotor and 3500 kN weight of tower. The weight of the ballast and the draft of the spar are adjusted in such a way to keep the centre of gravity below the centre of buoyancy. The mooring lines are divided into four groups, each of which has four lines. The studies were carried out in regular and random waves. The operational significant wave height of 2.5 m and 10 s wave period and survival significant wave height of 6 m and 18 s wave period in 300 m water depth are considered. The wind speed corresponding to the operational wave height is about 22 knots and this wind speed is considered to be operating wind speed for turbines. The heave and surge accelerations at the top of spar platform were measured and are used for calculating the response. The geometric modeling of spar was carried out using Multisurf and this was directly exported to WAMIT for subsequent hydrodynamic and mooring system analysis. The numerical results were compared with experimental results and the comparison was found to be good. Parametric study was carried out to find out the effect of shape, size and spacing of keel plate and from the results obtained from present work, it is recommended to use circular keel plate instead of square plate.

**Keywords:** spar platform; wind turbine; keel plate; slack mooring; regular waves; random waves.

---

### 1. Introduction

Among all renewable energy sources, wind has the potential to make the most significant contribution (Roddier 2009). Wind turbine technology is mature and bankable, and wind resources around the world are abundant. The wind turbines can be efficiently used in offshore, where the wind is stronger and more consistent. When hydrocarbons were found in very deep waters the oil and gas industry turned to floating platforms. The offshore wind turbines inherently have large mass

---

\* Corresponding author, Research scholar, E-mail: [seebai7@yahoo.co.in](mailto:seebai7@yahoo.co.in)

in the nacelle and rotor at an elevation of 80 to 100 meters above sea level, stability of floating platform is a challenge. Three options are there for stability while going to deeper waters (1) Keeping the centre of gravity of the platform as low as possible, this calls for very deep hull which is possible in spars (2) Providing mooring lines which will give external stability (3) keeping the floater surface area at the free surface wide i.e., to have large geometrical inertia which is possible in semi-submersible and TLP. In wind power industry, water depth is described in three distinct zones: shallow (less than 20 meters deep), transitional (20 to 50 meters), deep (greater than 50 meters). Fixed monopole structures are suitable up to a water depth of 30 meters, i.e., for 1-2 MW wind turbine. Jacket structures can be used up to 50 meters, for 2-4 MW and other floating structures like spars, semi submersibles and TLP's beyond 120 meters. A key task of the spar design to support the wind turbine is the selection of the optimal combination of floater shape and size, amount of ballast and mooring system attributes (Figs 1(a) and 1(b)) in order to keep the floater responses and nacelle acceleration within acceptable bounds and also to reduce the construction and installation costs. The experimental and numerical studies on the hydrodynamic response of a spar with 5 MW floating wind turbine are presented in this paper. A 1 : 100 scale model of the spar is studied in the wave basin for three configurations. A photo of the model is given in Fig. 2(a). The numerical modeling was done using software Multisurf (2009) and the hydrodynamic analysis using software WAMIT (2010).

The following literatures were reviewed to get an idea about response of a various floating platforms in regular and random waves. Chitrapu *et al.* (1998) studied the motion response of a spar platform in different environmental conditions using time domain simulation. Fisher *et al.* (1998) studied the heave characteristics of spar platform numerically and experimentally. Henderson *et al.* (2004) studied about floating wind farms for shallow offshore sites. Musial *et al.* (2004) provided a framework for the classification of floating wind turbine platforms and first-order economic analysis

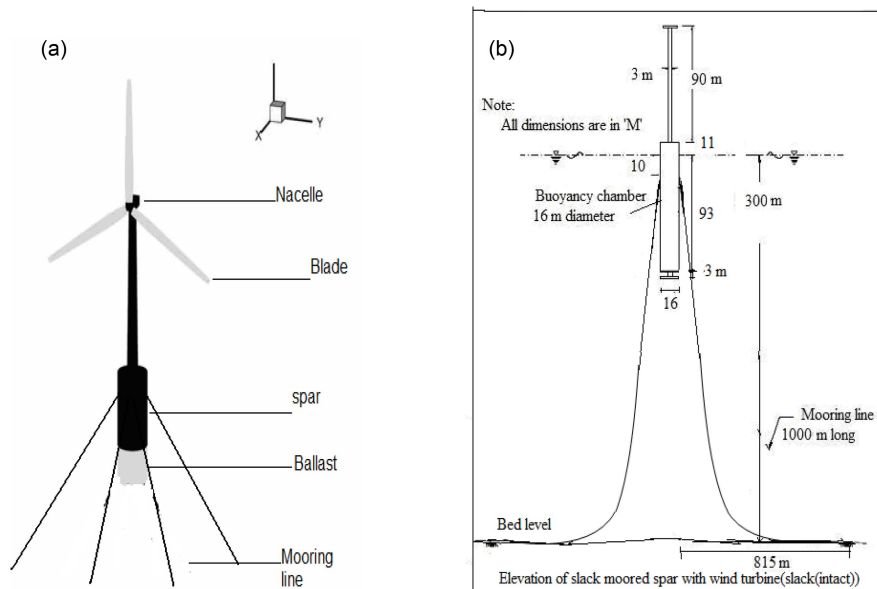


Fig. 1 (a) Spar with wind tower and (b) prototype details of sparD- slack mooring condition

on a wide range of platform architectures. Scлавounos *et al.* (2007) conducted a fully coupled dynamic analysis of floating wind turbines that enabled a parametric design study of a few floating wind turbine concepts and mooring systems. The limiting heave acceleration is reported as 0.5 g in his paper. Tracy (2007) have reported that the wind turbine will lose its efficiency beyond a heel angle of 10 degree. Wayman (2006) took some early steps towards the development of innovative and cost effective floating platforms to support a 5 MW wind turbine for deployment in water depths of 30-300 meters. In all the above studies deep draft spar buoy has not been considered with keel plates. The deep draft buoy of about 90 m equivalent to the height of wind turbine will keep the centre of gravity as low as possible whereas the keel plate will increase the added mass and damping. The geometry and ballast of the spar can be adjusted to achieve the required restoring moment against the wind heeling moment for heel angle less than 2 degree. However the wave forces on the spar will be critical and the keel plate and appropriate mooring system will be effective to reduce the pitch and heave. The pitch angle of less than 5 degree and heave acceleration of less than 0.2 g is recommended for offshore platforms. It is planned to limit the pitch angle to less than 5 degree and heave acceleration less than 0.2 g due to wave alone so that the pitch and heave due to combined effect of wind and wave will be less than the limits of 10 degree and 0.5 g. The significant wave height in the range of 2.5 m to 9 m at 4.5 to 18 s period ranges is likely to occur for the wind speed in the range of 22 knots to 40 knots, the operating wind speed for wind turbine. The wind force acting on tower is not considered in the present study, as the wave basin is not equipped with wind generation capability. Hence it is proposed to study the effect of keel plate and slack mooring on spar motion in regular and random waves and the effect of wind are not considered.

The objective of this work is to carryout the response analysis of a slack moored spar platform with bottom keel plates to support a 5 MW wind turbine, using experimental and numerical studies.

## 2. Design of spar

The spar is designed for an operational wave height of 4.5 m at the wave period of 10 s. In order to restrict the heave acceleration well below 0.2 g in operational sea state and 0.5 g in extreme sea state the heave natural period is aimed at 20 s, far away from the operational wave period. The pitch natural period for spar is about twice the heave period and hence the pitch angle also will be less than 2 degree in operational sea state and 5 degree in extreme sea state since the pitch period will be significantly more than the wave period. The 16 m diameter and about 95 m draft spar with 18,500 tons displacement is designed in such a way that the pitch period of about 50 s and heave period of 20 s is obtained. The mooring system is designed with 16 mooring lines each of length 1000 m in four groups with each group having 4 lines. The submerged weight of each mooring line is 42.59 kg/m and breaking strength is 7486 KN. The fairlead point is located 10 m below the water level.

## 3. Experimental studies

The physical model in 1:100 scale was tested in the wave basin in Ocean engineering department, IIT Madras. The wave basin is 30 m long, 30 m wide and 3 m deep (Fig. 2(b)). The model was fixed at a distance of 8 m from Multi element wave makers. The physical model of the

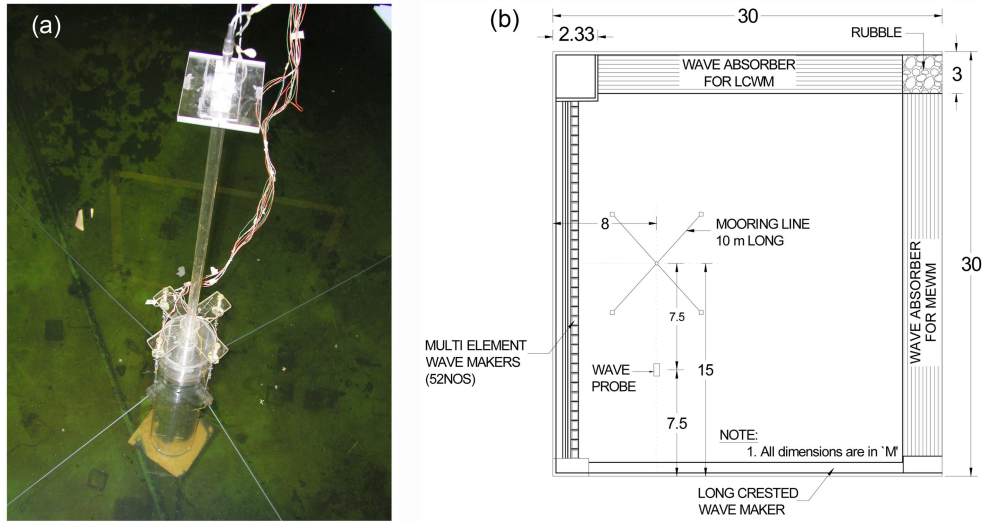


Fig. 2(a) Photo of spar model with square plate at bottom and (b) spar model in the wave basin

Table 1. Spar platform for wind turbine with slack mooring configuration

Description	sparD		sparCD		sparSD	
	Proto type	Model (1:100)	Proto type	Model (1:100)	Proto type	Model (1:100)
Displacement	18475 Ton	18.475 kg	18589 Ton	18.589 kg	18287.4 Ton	18.287 kg
Total weight of structure	184650 kN	184.65 N	185790 kN	185.79 N	182790 kN	182.79 N
Total pretension( $T_t$ )	100 kN	0.1 N	98 kN	0.098 N	84 N	0.084 N
$T_t/D$	0.054%	0.054%	0.052%	0.052%	0.05%	0.05%
Tower weight+ Nacelle and rotor $w_t$	7187 kN	7.18 N	7187 kN	7.18 N	7187 kN	7.18 N
Free board	11 m	0.11 m	11 m	0.11/m	12 m	0.12 m
Draft	95 m	0.95 m	95.5 m	0.955 m	94 m	0.94 m
Water depth	300 m	3 m	300 m	3 m	300 m	3 m
Height of spar	106 m	1.06 m	106.5 m	1.065 m	106 m	1.06 m
Diameter of spar	16 m	0.16 m	16 m	0.16 m	16 m	0.16 m
VCG	36.4 m	0.364 m	35.36 m	0.3536 m	35.87 m	0.3587 m
VCB	47.5 m	0.475 m	47.75 m	0.478 m	47 m	0.47 m
GM	11.3m	0.113 m	12.56 m	0.1256 m	11.3 m	0.113 m
Number/length of mooring line	16No/1000 m	4 No/10 m	16No/1000 m	4No/10 m	16No/1000 m	4No/10 m
$W_t$ of mooring in water	42.59 kg/m	18.27 g/m	42.59 kg/m	18.27 g/m	42.59 kg/m	18.27 g/m

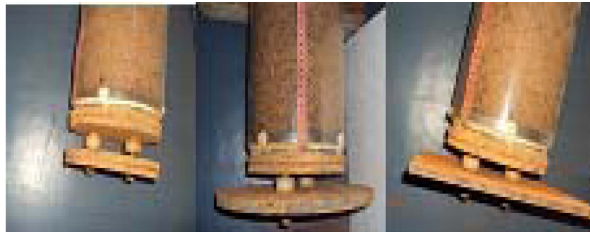


Fig. 3 Spar experimental model with keel plates (sparD, sparCD, sparSD)

spar along with the mooring details in wave basin is shown in Figs. 1(a) and 1(b). The basic dimensions, structural properties and mooring details of the model are given in Table 1.

The experimental studies were carried out for three configurations sparD, sparCD and sparSD. In all the configurations keel plate is placed at a distance of 3 cm from the bottom of the spar. In the configuration sparD the circular keel plate is having the same diameter of spar whereas for the configuration sparCD, the circular plate diameter is 24 cm and for sparSD, a square keel plate of  $24 \times 24$  cm is provided (Fig. 3). The horizontal distance of the touch down point of the 10 m long mooring lines from the spar is 8.15 m.

### 3.1 Free decay test

Free decay tests in heave response was obtained in the wave basin for all the three configurations i.e., sparD, sparCD and sparSD, wherein the spar was subjected to an initial heave offset and a sudden release; the resulting motions were monitored using accelerometers. Analysis of the heave decay curve shows that the heave natural period in model is 1.95 seconds for sparD and sparCD and 2.2 s for sparSD since the total mass of structure is kept same in all the three configurations, whereas the damping factor is obtained as 2.57% for sparD, 2.507% for sparCD and 2.36% for sparSD configuration, whereas the corresponding still water damping in surge is 0.867% for sparD, 0.768% for sparCD and 0.86% for sparSD configuration. The least square fit of the decay amplitudes is reasonably linear indicating that the damping due to the free oscillation of the model is essentially linear.

### 3.2 Response amplitude operator

The measurements have been taken for regular waves with wave heights of about 6 cm for the duration of 40 s with a sampling time interval of 0.05 s. The arrival time of the wave at the model depends on the wave frequency, and hence each time series of waves and acceleration responses have been analyzed separately. The incident wave and acceleration responses are calculated by averaging the crest to trough height of three steady response cycles just after the transient response. The wave and response records were collected for 70 s with a sampling interval of 0.05 s for random wave tests. After removing the transient response, the effective record length of time series available is 60 s. The time series is subjected to the Fast Fourier Transform, FFT to obtain the wave and response spectra using software MATLAB (2004).

The response of the body in regular waves can generally be expressed in terms of response amplitude operator as given in Eqs. (1) and (2). *RAO* is defined as the response of the structure due to a unit amplitude wave.

$$RAO_1(\omega) = \frac{\delta_1}{H/2} \quad (1)$$

$$RAO_2(\omega) = \frac{\delta_2}{H/2} \quad (2)$$

Where  $\delta_1$  and  $\delta_2$  is the response amplitude in the surge and heave mode due to wave height of  $H$ .

The response amplitude operator for the random wave tests can be estimated from the measured acceleration spectrum,  $S_{Mf}(\omega)$  and the incident wave spectrum,  $S\eta(\omega)$  as given in Eq. (3).

$$RAO_j(\omega) = \sqrt{\left(\frac{S_{Mf}(\omega)}{\omega^4 \times S\eta(\omega)}\right)} \quad j = 1,2 \quad (3)$$

#### 4. Numerical studies

The discretization of the submerged portion of the spar using Multisurf is shown in Fig. 4(a) for all the three configuration. WAMIT incorporating the mooring effect by external stiffness is used for the numerical analysis. The mooring stiffness is calculated using the stiffness equation suggested by Patel and Lynch (1984).

WAMIT uses the diffraction and the added mass and damping coefficient arise from radiation forces, whereas the exciting forces are of the diffraction type. WAMIT analysis using radiation damping alone is over predicting the response. The radiation damping is found to be less than the damping obtained in free decay tests and hence additional damping was added but this also over predicts the response beca use the amplitude of motion in free decay test is much less compared to amplitude of motion in regular and random wave test. Hence additional damping was increased to twice the free decay test and the comparison is found good.

The parametric studies have been carried out for all 3 configurations with slack mooring by varying the damping ratio and spacing of keel plate. The keel plate spacing is varied as 0.1875D,

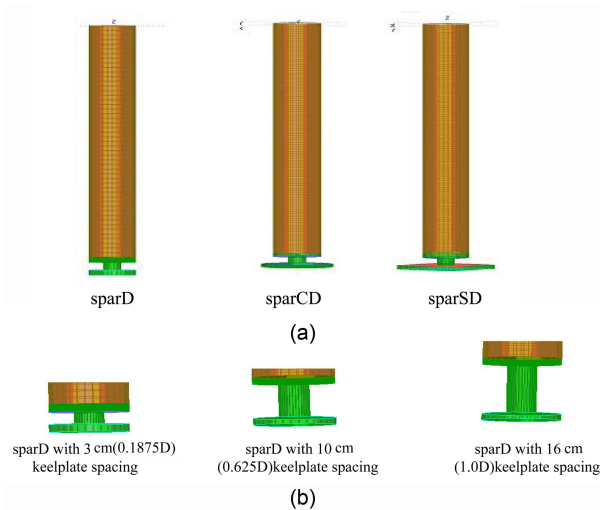


Fig. 4 (a) Numerical model of sparD, sparCD, sparSD and (b) keel plate spacing of sparD (numerical model)

0.625D and D, where D is the diameter of spar and the details are shown in Fig.4(b). The response of sparCD with circular keel plate of diameter 1.7D and sparSD with square keel plate of (1.5D × 1.5D) are shown in Figs. 11(a) and 11(b). In both the cases the keel plate area is same.

### 5. Results and discussions

#### 5.1 Validation of numerical results with experimental results

A comparison was made between experimental and numerical results for all 3 configurations. Comparison of surge and heave *RAO* for 3 configurations in regular and random waves with slack mooring is given in Figs. 5-7. The parametric study is carried out for seeing the effect of damping on heave *RAO* by increasing the damping as 1, 2, 3, 5, 7 and 10 times the free oscillation damping and the comparison of experimental and numerical results were found good for twice the free oscillation damping. The response in the long period range is inevitably corrupted by wave

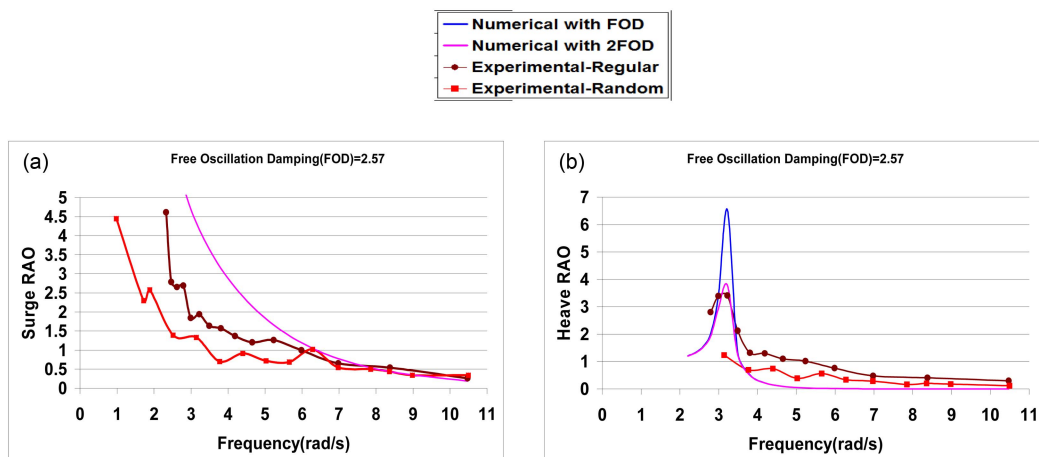


Fig. 5 (a) Surge *RAO* Vs Frequency for sparD with slack mooring (model scale) and (b) Heave *RAO* Vs Frequency for sparD with slack mooring (model scale)

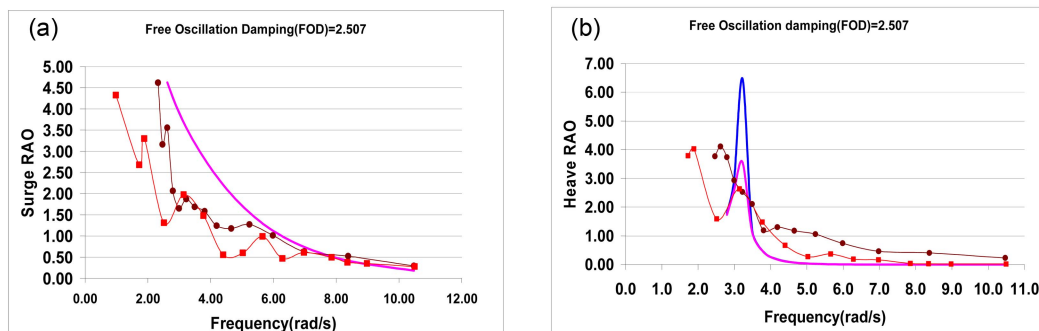


Fig. 6 (a) Surge *RAO* Vs Frequency for sparCD with slack mooring (model scale) and (b) Heave *RAO* Vs Frequency for sparCD with slack mooring (model scale)

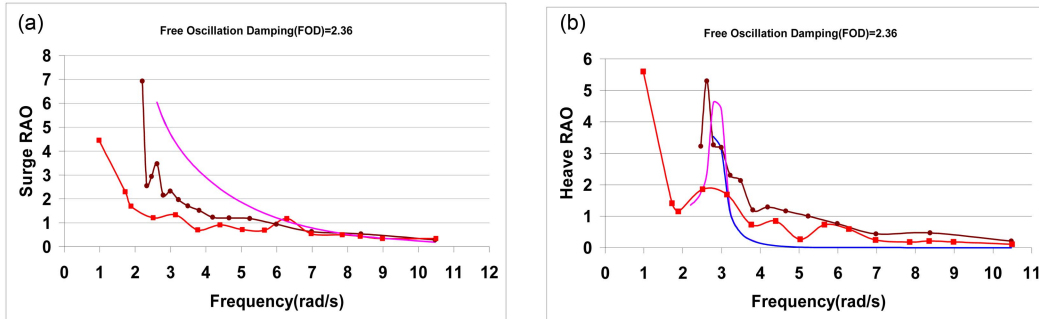


Fig. 7 (a) Surge *RAO* Vs Frequency for sparSD with slack mooring (model scale) and (b) Heave *RAO* Vs Frequency for sparSD with slack mooring (model scale)

reflections in the test basin, so for comparison purpose experimental readings were taken up to the heave natural period. If the system is linear, regular *RAO* and random *RAO* will be same, but the proposed spar buoy system is nonlinear and hence the regular and random *RAO* does not match.

5.2 Parametric study

5.2.1 Effect of spacing of keel plate

The heave and surge *RAO* for all 3 configurations with 3 different spacing of 0.1875D, 0.625D and D obtained at the top of the platform was given in Figs. 8-10. The increase in keel plate spacing decreases heave *RAO* up to spacing equal to half the diameter of spar and after that heave *RAO* increases. But the increase in keel plate spacing results in decrease in surge *RAO*.

5.2.2 Effect of shape of keel plate

The response of sparCD with circular keel plate of diameter 1.7D and sparSD with square keel plate of (1.5D × 1.5D) obtained at the top of platform are shown in Figs. 11(a) and 11(b). In both the cases the keel plate area is same. The heave and surge *RAO* are found to be higher for sparSD

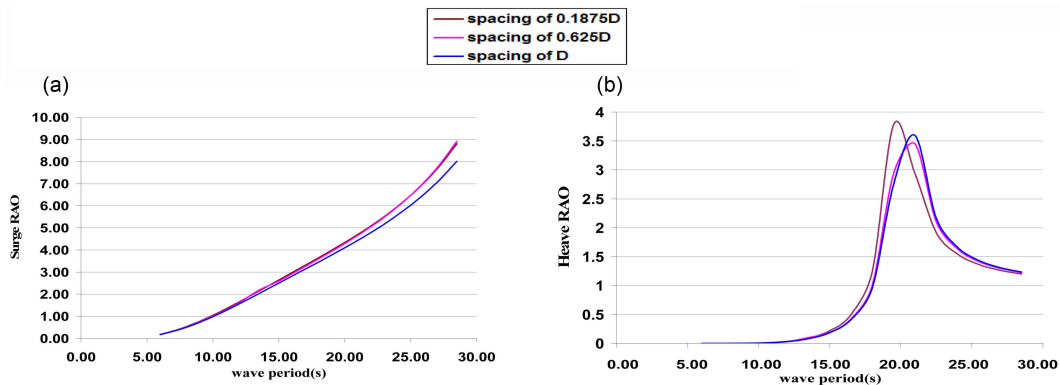


Fig. 8 (a) Surge *RAO* Vs wave period for sparD configuration for keel plate spacing of 0.1875D, 0.625D, D (prototype scale) and (b) Heave *RAO* Vs wave period for sparD configuration for keel plate spacing of 0.1875D, 0.625D, D (prototype scale )

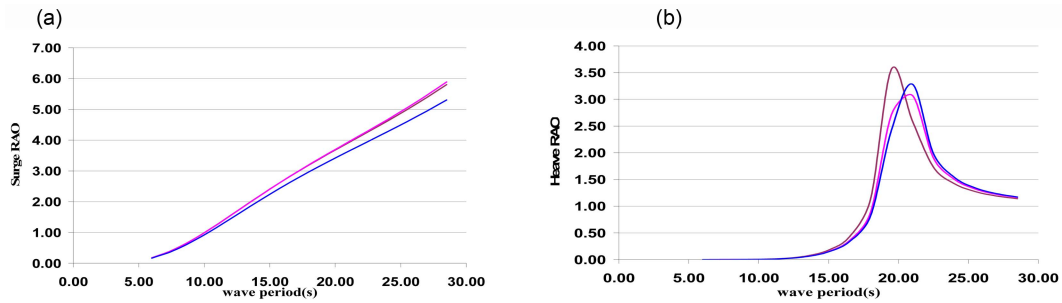


Fig. 9 (a) Surge *RAO* Vs wave period for sparCD configuration for keel plate spacing of 0.1875D, 0.625D, D (prototype scale) and (b) Heave *RAO* Vs wave period for sparCD configuration for keel plate spacing of 0.1875D, 0.625D, D (prototype scale)

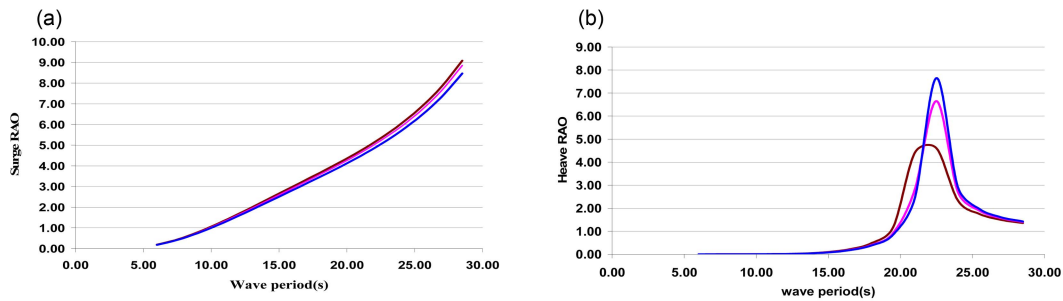


Fig. 10 (a) Surge *RAO* Vs wave period for sparSD configuration for keel plate spacing of 0.1875D, 0.625D, D (prototype scale) and (b) Heave *RAO* Vs wave period for sparSD configuration for keel plate spacing of 0.1875D, 0.625D, D (prototype scale)

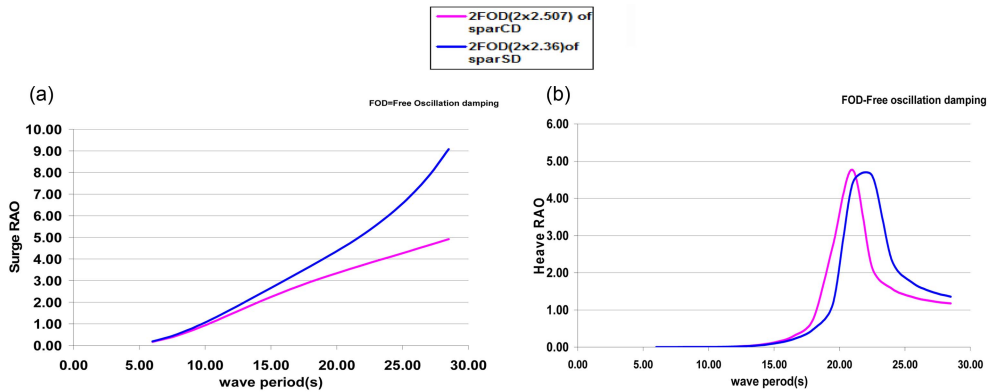


Fig. 11 (a) Surge *RAO* Vs wave period (s) (prototype scale) and (b) Heave *RAO* Vs wave period (s) (prototype scale)

compared to sparCD of same keel plate area.

### 5.2.3 Effect of oblique wave

The comparison of surge and heave *RAO* at the top of platform obtained for 0 and 45 degree oblique waves for sparD, sparCD and sparSD was carried out and results of sparD is shown in Fig. 12. The

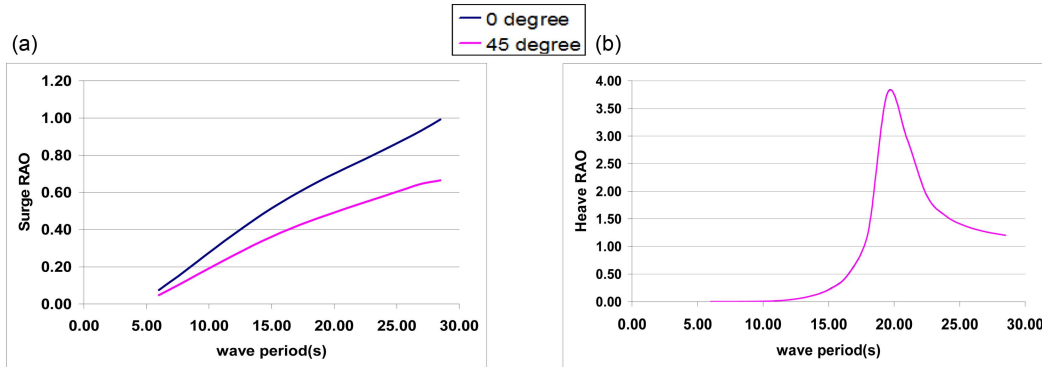


Fig. 12 (a) Surge *RAO* Vs wave period for sparD (Prototype scale) and (b) Heave *RAO* Vs wave period for sparD (Prototype scale)

results indicates that surge *RAO* for all 3 configurations are less in 45 degree waves compared to that in 0 degree waves whereas in Heave *RAO* the effect of direction of waves is negligible.

#### 5.2.4 Effect of wave height

The wave heights and wave periods are obtained from corresponding wind speed as shown in Fig. 13. The studies are carried out up to a wind speed of 25 m/s, because beyond 25 m/s is considered as cut-out wind speed where the wind turbine ceases to generate electricity. The RMS value of heave nacelle acceleration in %g was obtained for sparD, sparCD and sparSD configuration with slack mooring at different sea state (Table 2), where the PM spectrum of different wave heights are multiplied with *RAO* obtained from present study to get the heave nacelle acceleration at different sea state and the results were found less than the permitted 10%g in offshore wind turbines. Heave *RAO* at natural period is obtained from Figs. 5(b), 6(b) and 7(b).

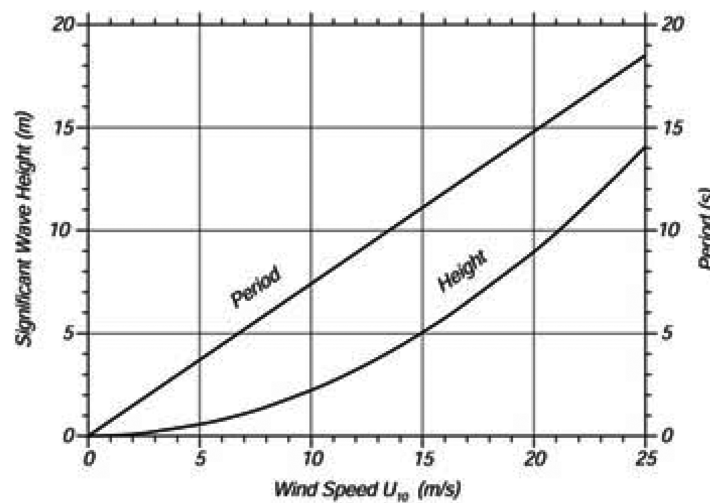


Fig. 13. Significant wave-height and period calculated from the Pierson-Moskowitz spectrum (Ref: 10)

Table 2 Response corresponding to wind speeds 10, 15, 20 and 25 m/s

Significant wave height(Hs),wave period(Tp),wind speed(V)	RMS of nacelle acceleration in %g(heave acceleration)			Heave <i>RAO</i> at natural period		
	sparD	sparCD	sparSD	sparD	sparCD	sparSD
Hs=2.5 m,Tp=7.5 s,V=10 m/s	0.86	0.93	0.96	3.39	2.94	3.19
Hs=5 m,Tp=11.5 s,V=15 m/s	0.63	0.68	0.70	3.39	2.94	3.19
Hs=9 m,Tp=15 s,V=20 m/s	0.71	0.77	0.79	3.39	2.94	3.19
Hs=14 m,Tp=18.5 s,V=25 m/s	0.77	0.83	0.85	3.39	2.94	3.19
Hs=6 m,Tp=10 s,V=11.4 m/s (Experimental results)	0.69	0.67	0.67	3.39	2.94	3.19

## 6. Conclusions

(i) The surge and heave *RAO* obtained by experimental studies do not compare well with the numerical results, since the WAMIT analysis considers only radiation damping. So additional damping obtained from free oscillation tests was added but this also over predicts the response because the amplitude of motion in free vibration analysis is much less compared to amplitude of motion during forced response analysis. Hence additional damping was increased to twice the free oscillation damping and the comparison with experimental results found good.

(ii) The addition of square keel plate with same area as that of circular keel plate results in increase in heave *RAO* due to increase in heave exciting force on the square plate and hence it is recommended to use circular keel plate.

(iii) In sparCD, the increase in keel plate spacing decreases heave *RAO* due to increase in damping. However the decrease is marginal when the spacing is increased beyond half the diameter of the spar and hence the keel spacing of half the diameter is recommended whereas increase in spacing in case of sparSD configuration results in increase on heave *RAO* and heave natural period due to increase in added mass.

(iv) The response for different wave heights corresponding to different wind speeds 10, 15, 20 and 25 m/s shows that present design can withstand wave heights and wave periods for all wind speeds.

## References

- Chitrapu, A.S., Saha, S. and Salpekar, V.Y. (1998), "Time domain simulation of spar platform response in random waves and current", ASME, OMAE98-0380, 1–8.
- Fischer, F.J. and Gopalkrishnan, Ram. (1998), "Some observations on the heave behaviour of spar platforms", *J. Offshore Mech. Arct.*, **120**(4), 221–225.
- Henderson, A.R., Zaaijer, M.B., Builder, B., Pierik, J., Huijsmans, R., Vanhees, M., Snijders, E. and Wolf, M.J. (2004), "Floating Wind Farms for Shallow Offshore Sites", *Proceedings of the ISOPE conference*, Toulon, France.
- Musial, W., Butterfield, S. and Boone, A. (2004), "Feasibility of floating platform systems for wind turbines", *Proceedings of the 23rd ASME Wind Energy Symposium*, Reno, Nevada, USA.
- Patel, M.H. and Lynch, E.J. (1984), "Coupled dynamics of tensioned buoyant platforms and mooring tethers",

- Eng. Struct.*, **5**(4), 299-308.
- Roddier, Dominique., Cermelli, C. and Weinstein, A. (2009), "Wind float: Floating foundation for offshore wind turbines part1: Design basis and qualification process", ASME, OMAE09-79229.
- Sclavounos, P., Tracy, C. and Lee, S. (2007), *Floating offshore wind turbines: responses in a sea state pareto optimal designs and economic assessment*, Department of Mechanical Engineering, MIT, Cambridge, USA.
- Wayman, E.N. and Sclavounos, P.D. (2007), "Coupled dynamic modeling of floating wind turbine systems", OTC -18287, Houston, Texas, U.S.A..
- Tracy, C. (2007), *Parametric design of Floating wind turbine*, M.S.Thesis, Department of Ocean Engineering, Massachusetts Institute of Technology.
- Stewart, H.R (2005), *Introduction to Physical Oceanography*, Department of Oceanography, Texas A & M University, USA.
- Wayman, E.N. (2006), *Coupled dynamics and economic analysis of floating wind turbine systems*, M.S. Thesis, Department of Ocean Engineering, MIT, Cambridge, USA.
- MATLAB user manual (2004), Version 7.0.0.
- MULTISURF user manual (2009), Version 7.0.
- WAMIT user manual (2010), Versions 6.2, 6.2PC, 6.2S, 6.2S-PC.